DOI: 10.1002/ejic.200700020

Synthesis and Characterization of Iron, Cobalt, and Nickel Complexes Bearing Novel *N*,*N*-Chelate Ligands and Their Catalytic Properties in Ethylene Oligomerization

Li Wang,[a] Cheng Zhang,[a] and Zhong-Xia Wang*[a]

Keywords: Iron / Cobalt / Nickel / Catalysis / Ethylene / Oligomerization

Treatment of *o*-ROC_6H_4NC (R = $PhCH_2$, *i*Pr) with [Li{2-$CH(SiMe_3)C_5H_4N$}] afforded dimeric lithium complexes [Li{N(*o*-ROC_6H_4)$C(SiMe_3)CH(2$-$C_5H_4N)$}]$_2$ (**3**, R = $PhCH_2$; **4**, R = *i*Pr). Reaction of the lithium complexes with 1 equiv. of (dme)$NiCl_2$ gave nickel complexes [Ni{N(*o*-ROC_6H_4)-$C(SiMe_3)CH(2$-$C_5H_4N)$}$_2$] (**5**, R = $PhCH_2$; **6**, R = *i*Pr). The stoichiometric reaction of complexes **3** and **4** with $Et_3NH^+Cl^-$ formed 2-{*o*-$ROC_6H_4NHC(SiMe_3)CH$}C_5H_4N (**7**, R = $PhCH_2$; **8**, R = *i*Pr) in quantitative yields. Reaction of **7** or **8** with metal halides, including (dme)$NiCl_2$, $NiBr_2$, $FeCl_2{\cdot}4H_2O$, and $CoCl_2$ yielded complexes [MX_2{(*o*-ROC_6H_4)$N{=}C(SiMe_3)CH_2$(2-C_5H_4N)}] (**9**, R = $PhCH_2$, M = Ni, X = Cl; **10**, R = *i*Pr, M = Ni, X = Cl; **11**, R = $PhCH_2$, M = Ni, X = Br; **12**, R = *i*Pr, M = Ni, X = Br; **13**, R = $PhCH_2$, M = Fe, X = Cl; **14**, R = *i*Pr, M = Fe, X = Cl; **15**, R = $PhCH_2$, M = Co, X = Cl; **16**, R = *i*Pr, M = Co, X = Cl). For comparasion, nickel and cobalt complexes [MX_2{(*o*-MeC_6H_4)$N{=}C(SiMe_3)CH_2$(2-C_5H_4N)}] (M = Ni, X = Br, **18**; M = Co, X = Cl, **19**) were similarly synthesized through reaction of 2-{*o*-$MeC_6H_4NHC(SiMe_3)CH$}C_5H_4N (**17**) with $NiBr_2$ and $CoCl_2$, respectively. These compounds were characterized by NMR (for **3**, **4**, **7**, **8**, and **17**) and IR (for **5**–**19**) spectroscopy, elemental analyses and HRMS (for **5**, **6**, and **9**–**19**). The molecular structures of complexes **3**, **6**, **12**, and **14** were characterized by single-crystal X-ray diffraction techniques. The catalytic behavior in ethylene oligomerization of complexes **5**, **6**, **9**–**16**, **18**, and **19** was investigated. Under optimal conditions, the complexes showed good catalytic activities upon activation with appropriate aluminum co-catalysts (8.72×10^2 to 18.2×10^2 kg/mol h atm for the nickel complexes upon activation with Et_2AlCl and 4.3×10^2 to 8.1×10^2 kg/mol h atm for the iron and cobalt complexes upon activation with MMAO).

Introduction

Late-transition-metal complexes with *N*,*N*-chelate ligands have attracted considerable attention due to their catalytic actions, especially for developing non-metallocene catalysts for the polymerization of ethylene and α-olefins.[1] Following the pioneering studies of Keim and Fink,[1d,2] Brookhart and co-workers reported on the discovery of the α-diimine complexes of Ni^{II} and Pd^{II} catalysts for the polymerization of ethylene and α-olefins.[3] Subsequently, the number of academic publications and patents for polyolefins and oligomers obtained with late-transition-metal complexes increased remarkably.[1,4] A large number of structural variations of diimines have also been reported to adjust the steric and electronic properties of the *N*,*N*-chelate ligands.[1,5] These include β-diimines and analogues whose complexes of Ni^{II} and Pd^{II}, however, usually exhibit lower catalytic activities than the α-diimine complexes.[1a,6] A further modification is to append a donor sidearm, constructing tridentate chelating ligands such as *N*,*N*,*O*,[7] *N*,*N*,*P*,[8] and *N*,*N*,*N* ligands.[9] A representative example are bis(imino)pyridine ligands whose iron complexes showed exceptionally high activities for ethylene polymerization when activated with MAO.[10]

Furthermore, late-transition-metal complexes could act as better candidates for ethylene oligomerization because of their facile β-H elimination.[11] Many neutral and cationic late-transition-metal complexes with chelate ligands have been successfully applied in the field of olefin oligomerization.[12,13] The Shell Higher Olefin Process (SHOP) is an excellent example. However, the demand for linear α-olefins in the C_4–C_{10} range is growing fast. Much effort is still devoted to the development of highly selective ethylene oligomerization catalysts, and identifying and fine-tuning the parameters that influence the activity and selectivity of suitable catalysts continues to represent a challenge.[13] Our current efforts focus on the synthesis of new functional ligands and their corresponding late-transition-metal complexes as well as the catalytic behavior for ethylene oligomerization. Herein, we report on the synthesis and characterization of new ligands and their lithium and late-transition-metal complexes, while their catalytic behavior for ethylene oligomerization was also investigated and discussed.

[a] Department of Chemistry, University of Science and Technology of China,
Hefei, Anhui 230026, P. R. China

Results and Discussion

Synthesis and Characterization

Compounds **1** and **2** were prepared according to a literature method.[14] Syntheses of **3**–**16** are summarized in Scheme 1. Reaction of *o*-ROC_6H_4NC (R = $PhCH_2$, *i*Pr) with [Li{2-$CH(SiMe_3)C_5H_4N$}] afforded dimeric lithium complexes [Li{$N(o\text{-}ROC_6H_4)C(SiMe_3)CH(2\text{-}C_5H_4N)$}]$_2$ (**3**, R = $PhCH_2$; **4**, R = *i*Pr) as yellow, air-sensitive solids. In the reaction, a 1,2-$SiMe_3$ migration from the α- to the β-carbon atom took place. This type of reaction between an isocyanide and (trimethylsilyl)methyllithium has been reported.[15] Reaction of **3** and **4** with 1 equiv. of (dme)$NiCl_2$ gave nickel complexes [Ni{$N(o\text{-}ROC_6H_4)C(SiMe_3)CH(2\text{-}C_5H_4N)$}$_2$] (**5**, R = $PhCH_2$; **6**, R = *i*Pr). Attempts to synthesize [NiCl{$N(o\text{-}ROC_6H_4)C(SiMe_3)CH(2\text{-}C_5H_4N)$}] by reaction of **3** or **4** with various amounts of (dme)$NiCl_2$ were unsuccessful. Complexes **3** and **4** were treated with 1 equiv. of $Et_3NH^+Cl^-$ to afford 2-{*o*-$ROC_6H_4NHC(SiMe_3)CH$}C_5H_4N (**7**, R = $PhCH_2$; **8**, R = *i*Pr) as a pale yellow solid (**7**) or a yellowish oil (**8**), each existing in an enamine form. Reaction of **7** or **8** with metal halides, including (dme)$NiCl_2$, $NiBr_2$, $FeCl_2{\cdot}4H_2O$ and $CoCl_2$, yielded [MX_2{$(o\text{-}ROC_6H_4)N{=}C(SiMe_3)CH_2(2\text{-}C_5H_4N)$}] (**9**, R = $PhCH_2$, M = Ni, X = Cl; **10**, R = *i*Pr, M = Ni, X = Cl; **11**, R = $PhCH_2$, M = Ni, X = Br; **12**, R = *i*Pr, M = Ni, X = Br; **13**, R = $PhCH_2$, M = Fe, X = Cl; **14**, R = *i*Pr, M = Fe, X = Cl; **15**, R = $PhCH_2$, M = Co, X = Cl; **16**, R = *i*Pr, M = Co, X = Cl). Compound **17** was prepared with a similar procedure as for **7** and **8** (Scheme 2). Thus, reaction of *o*-MeC_6H_4NC with [Li{2-$CH(SiMe_3)C_5H_4N$}] in Et_2O gave the lithium complex [Li{$N(o\text{-}MeC_6H_4)C(SiMe_3)CH(2\text{-}C_5H_4N)$}], which was hydrolyzed directly by treatment with 1 equiv. of water to afford neutral enamine **17**. Complexes **18** and **19** were synthesized through reaction of **17** with $NiBr_2$ or $CoCl_2$ in thf, just as for complexes **9**–**16**.

Complexes **3** and **4** were fully characterized by ^1H and ^{13}C NMR spectroscopy and elemental analyses. The data are consistent with their respective structure. Complexes **5** and **6** are paramagnetic and were characterized by IR spectroscopy, elemental analyses, and high-resolution mass spectrometry. Compounds **7** and **8** were characterized by ^1H, ^{13}C NMR, and IR spectroscopy and elemental analyses. The ^1H NMR spectra of **7** and **8** exhibit NH proton signals at δ = 11.77 and 11.58 ppm, respectively, and ethenyl proton signals at δ = 5.69 and 5.59 ppm, respectively. Their ^{13}C NMR spectra also show the existence of the C–C double bonds. These data prove the enamine forms of **7** and **8**. The similar compound **17** also exists in an enamine form, being a mixture of (*Z*) and (*E*) isomers. It was characterized by ^1H NMR and IR spectroscopy and high-resolution mass spectrometry. Complexes **9**–**16**, **18**, and **19** are crystalline solids or powders and paramagnetic; the complexes are yellow (**9**, **13**, and **14**), purple (**10** and **18**), red (**11** and **12**), or blue (**15**, **16**, and **19**). They gave satisfactory elemental analyses and high-resolution mass spectra. The IR spectra show C=N double-bond absorptions, proving

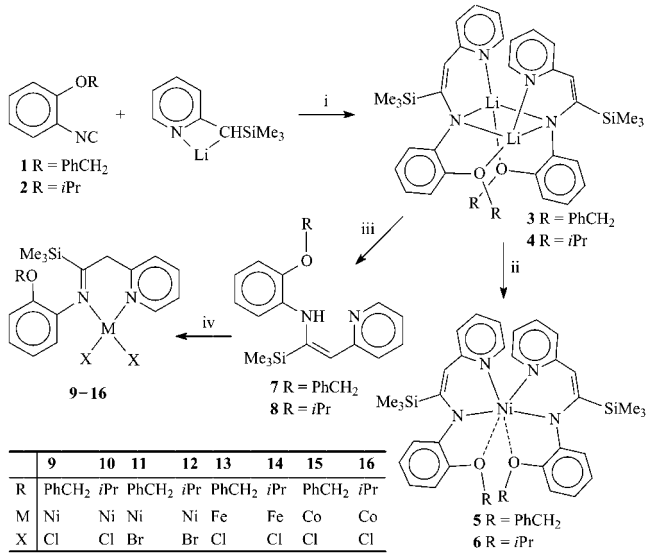

	9	10	11	12	13	14	15	16
R	$PhCH_2$	*i*Pr	$PhCH_2$	*i*Pr	$PhCH_2$	*i*Pr	$PhCH_2$	*i*Pr
M	Ni	Ni	Ni	Ni	Fe	Fe	Co	Co
X	Cl	Cl	Br	Br	Cl	Cl	Cl	Cl

Scheme 1. Synthesis of compounds **3**–**16**. Reagents and conditions: i: Et_2O, –30 °C to room temperature, 15 h; ii: (dme)$NiCl_2$, thf, –80 °C to room temperature, 15 h; iii: $Et_3NH^+Cl^-$, toluene, 0 °C to room temperature, 20 h; iv: L^1MX_2 [L^1MX_2 = (dme)$NiCl_2$, $NiBr_2$, $FeCl_2{\cdot}4H_2O$, $CoCl_2$], thf, 0 °C to room temperature, 15 h.

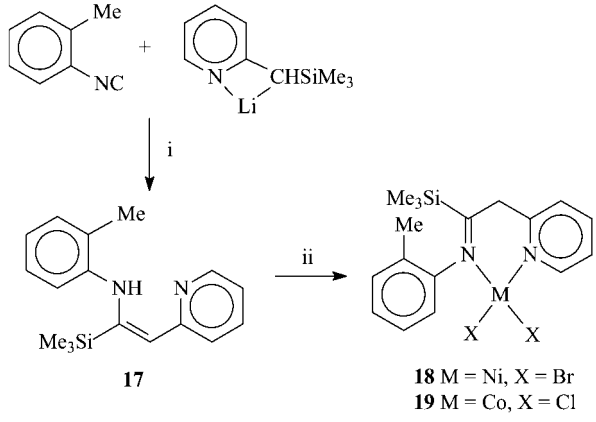

Scheme 2. Synthesis of compounds **17**–**19**. Reagents and conditions: i: Et_2O, –30 °C to room temperature, 15 h, and then H_2O, thf, 0 °C to room temperature, 10 min.; ii: $NiBr_2$ or $CoCl_2$, thf, 0 °C to room temperature, 15 h.

the coordinated ligands as imine forms in the complexes. This is also consistent with the single-crystal X-ray diffraction results of complexes **12** and **14**.

Complexes **3**, **6**, **12**, and **14** were further characterized by single-crystal X-ray diffraction techniques. The structure of complex **3** is presented in Figure 1 along with selected bond lengths and bond angles. The structure shows that complex **3** is dimeric in the solid state, in which two lithium atoms are bridged by two enamine nitrogen atoms, forming a 1,3-Li_2N_2 four-membered ring. With the 1,3-Li_2N_2 ring as the base, the NC_3NLi and NC_2OLi rings form the flaps of an "open-box"-like structural framework, in which each four-coordinate lithium atom has a distorted tetrahedral geometry. The Li–N distances from 1.967(8) to 2.108(8) Å are in the normal range. For example, the Li–N distances in

$[Li\{N(SiMe_3)C(R^2)C(R^1)(C_5H_4N\text{-}2)\}]_2$ (R^1 = H, R^2 = *t*Bu; R^1 = $SiMe_3$, R^2 = Ph) vary from 1.968(6) to 2.032(6) Å, and in $[Li\{N(SiMe_3)C(Ph)\}_2CH]_2$ from 1.952(10) to 2.095(2) Å.[16]

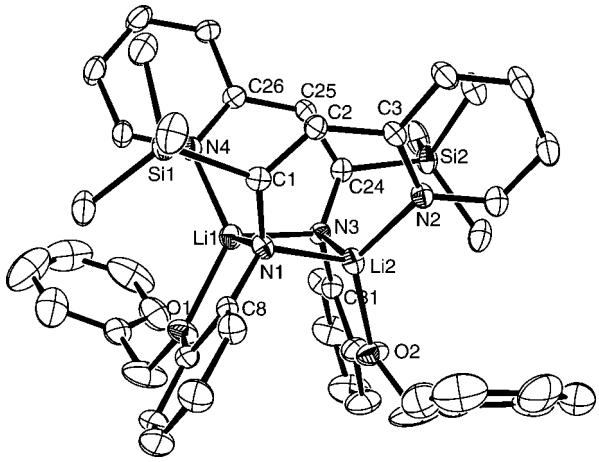

Figure 1. ORTEP drawing of complex **3** with 30% probability thermal ellipsoids. Selected bond lengths [Å] and bond angles [°]: Li(1)–N(1) 2.108(8), Li(1)–N(3) 1.990(8), Li(1)–N(4) 1.967(8), Li(1)–O(1) 2.055(8), Li(2)–N(1) 2.016(8), Li(2)–N(2) 1.982(8), Li(2)–N(3) 2.072(8), Li(2)–O(2) 2.037(8), Li(1)–Li(2) 2.495(10), N(1)–C(1) 1.403(5), C(1)–C(2) 1.363(5), N(3)–C(24) 1.394(5), C(24)–C(25) 1.363(5); N(1)–Li(1)–N(3) 103.8(3), N(1)–Li(1)–N(4) 119.0(4), N(3)–Li(1)–N(4) 98.9(4), N(3)–Li(1)–O(1) 121.7(4), N(4)–Li(1)–O(1) 130.7(4), N(1)–Li(1)–O(1) 79.8(3), N(1)–Li(2)–N(2) 98.4(3), N(1)–Li(2)–N(3) 104.2(3), N(2)–Li(2)–N(3) 119.3(4), N(1)–Li(2)–O(2) 122.2(4), N(2)–Li(2)–O(2) 129.2(4), N(3)–Li(2)–O(2) 81.3(3), Li(1)–N(1)–Li(2) 74.4(3), Li(1)–N(3)–Li(2) 75.8(3).

The molecular structure of complex **6** is depicted in Figure 2 along with selected bond lengths and bond angles. In the structure, a noteworthy feature is the distances between the Ni atom and the oxygen atoms. The Ni···O distances (2.574 and 2.586 Å, respectively) are longer than the sum of the covalent radii, however, much shorter than the sum of the van der Waals radii.[17] Hence, interactions between the Ni atom and the O atoms should be present. In this case, the coordination geometry of the Ni atom can be regarded as a distorted octahedron. The N1,N4,O1,N2 atoms are approximately coplanar, the torsion angle of N1–N4–O1–N2 being 0.7°, while the Ni atom is out of the plane.

The molecular structure of complex **12** is depicted in Figure 3 along with selected bond lengths and bond angles. The crystalline complex **12** is monomeric and the Ni center is in a distorted tetrahedral environment. The Ni···O distance of 3.781 Å shows no interactions between the atoms. The six-membered metallacycle exhibits a boat conformation. This is very similar to that of $[CH_2\{C(Me)=NAr\}_2]NiBr_2$ (Ar = 2,6-*i*$Pr_2C_6H_3$).[6a] The C5,N1,N2,C7 atoms are approximately coplanar, the torsion angle being 1.5°. The distance of Ni1–N1 [1.986(3) Å] is slightly shorter than that of Ni1–N2 [1.993(3) Å], and both are close to those found in $[2\text{-}\{Ph_2P=N(2',6'\text{-}Me_2C_6H_3)\}\text{-}6\text{-}Me_3SiC_5H_3N]NiBr_2$ [1.996(8) Å] and $[2\text{-}(Ph_3P=NCH_2)\text{-}6\text{-}MeC_5H_3N]NiBr_2$ [1.983(3) Å],[18] and slightly shorter than those of

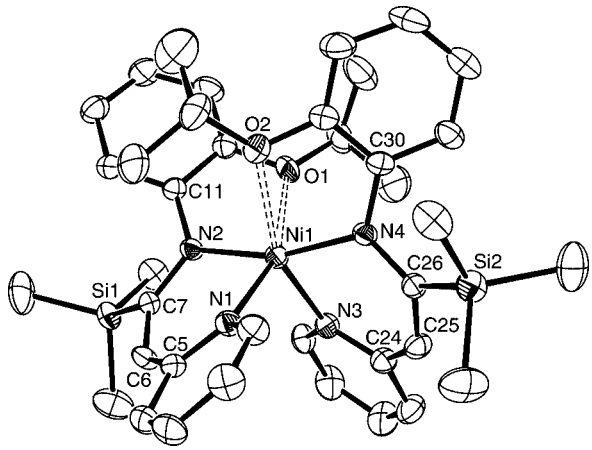

Figure 2. ORTEP drawing of complex **6** with 30% probability thermal ellipsoids. Selected bond lengths [Å] and bond angles [°]: Ni(1)–N(1) 2.045(3), Ni(1)–N(2) 1.968(3), Ni(1)–N(3) 2.043(4), Ni(1)–N(4) 1.976(3), Ni(1)···O(1) 2.574, Ni(1)···O(2) 2.586, C(6)–C(7) 1.377(6), C(25)–C(26) 1.371(6), N(2)–C(7) 1.377(5), N(4)–C(26) 1.373(5); N(1)–Ni(1)–N(2) 90.42(14), N(1)–Ni(1)–N(3) 100.11(14), N(1)–Ni(1)–N(4) 100.42(14), N(2)–Ni(1)–N(3) 100.77(14), N(2)–Ni(1)–N(4) 163.29(13), N(3)–Ni(1)–N(4) 89.88(14), O(1)–Ni(1)–N(1) 158.89, O(2)–Ni(1)–N(3) 158.58.

$[CH_2\{C(Me)=NAr\}_2]NiBr_2$ [2.010(5) and 2.022(5) Å, respectively].[6a] The Ni1–Br1 distance [2.3599(7) Å] is longer than that of Ni1–Br2 [2.3419(7) Å], and both are normal for four-coordinate Ni^{II} complexes.[19] The N2–C7 distance of 1.288(4) Å agrees with that of a C=N double bond, indicating that the enamine tautomerizes to an imine after coordination to Ni^{II}. The N1–Ni1–N2 bond angle of 91.76(12)° is close to that of $[CH_2\{C(Me)=NAr\}_2]NiBr_2$ [93.7(2)°].[6a] However, the Br1–Ni1–Br2 bond angle of 124.78(3)° is wider than that of $[CH_2\{C(Me)=NAr\}_2]NiBr_2$ [118.54(5)°].[6a]

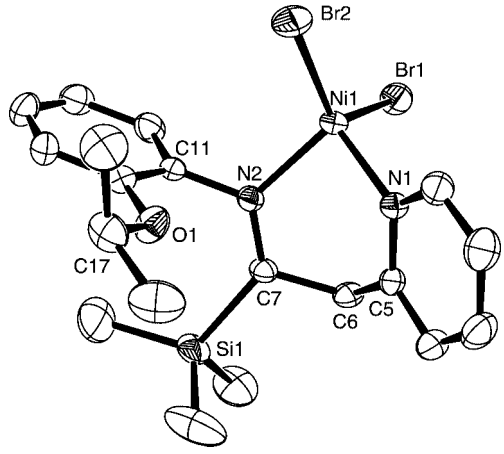

Figure 3. ORTEP drawing of complex **12** with 30% probability thermal ellipsoids. Selected bond lengths [Å] and bond angles [°]: Ni(1)–N(1) 1.986(3), Ni(1)–N(2) 1.993(3), Ni(1)–Br(1) 2.3599(7), Ni(1)–Br(2) 2.3419(7), Ni(1)···O(1) 3.781, C(5)–C(6) 1.501(6), C(6)–C(7) 1.527(5), N(2)–C(7) 1.288(4); N(1)–Ni(1)–N(2) 91.76(12), N(1)–Ni(1)–Br(1) 109.96(9), N(1)–Ni(1)–Br(2) 106.84(9), N(2)–Ni(1)–Br(1) 104.81(9), N(2)–Ni(1)–Br(2) 113.73(9), Br(1)–Ni(1)–Br(2) 124.78(3).

The structure of complex **14** is presented in Figure 4 along with selected bond lengths and bond angles. The crystalline **14** is monomeric and has a skeletal structure similar to that of **12**, including tetrahedral metal coordination geometry and the boat conformation of the six-membered metallacycle. The Fe1–N1 distance of 2.103(2) Å is slightly shorter than that of Fe1–N2 [2.115(2) Å], and both are within the normal range for this class of four-coordinate iron complexes. The Fe1–Cl1 distance of 2.2405(11) Å is longer than that of Fe1–Cl2 [2.2264(10) Å]. They are close to those in [2-{Ph_2P=N(2′,6′-$R'_2C_6H_3$)}-6-RC_5H_3N]$FeCl_2$ (R = Ph, $SiMe_3$; R′ = Me, *i*Pr) [2.2451(11)–2.2754(15) Å].[18] The Fe···O distance of 3.812 Å is beyond the distance of bonding interaction. The N2–C7 distance of 1.287(3) Å is almost the same as that of complex **12**, showing the ligand also to exist in an imine form.

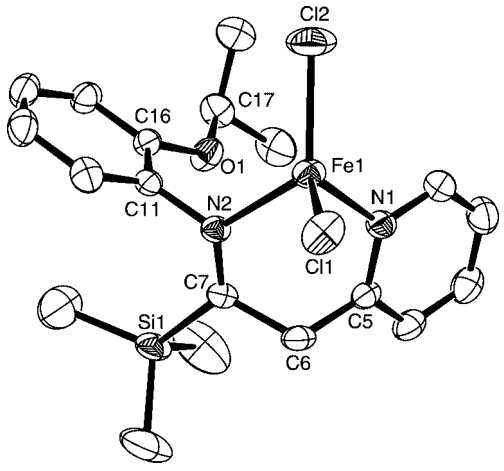

Figure 4. ORTEP drawing of complex **14** with 30% probability thermal ellipsoids. Selected bond lengths [Å] and bond angles [°]: Fe(1)–N(1) 2.103(2), Fe(1)–N(2) 2.115(2), Fe(1)–Cl(1) 2.2405(11), Fe(1)–Cl(2) 2.2264(10), Fe(1)···O(1) 3.812, N(2)–C(7) 1.287(3); N(1)–Fe(1)–N(2) 86.08(9), N(1)–Fe(1)–Cl(1) 112.84(7), N(1)–Fe(1)–Cl(2) 108.80(7), N(2)–Fe(1)–Cl(1) 108.49(7), N(2)–Fe(1)–Cl(2) 113.78(7), Cl(1)–Fe(1)–Cl(2) 121.39(4).

Catalytic Properties of Complexes 5, 6, 9–16, 18, and 19 for Ethylene Oligomerization

It has been reported that bis(chelate)nickel complexes can catalyze vinylic polymerization of norbornene, polymerization or oligomerization of ethylene or α-olefins in the presence of appropriate organoaluminum co-catalysts. Some showed high catalytic activity and good selectivity.[5f,20] We determined the catalytic activity for ethylene polymerization or oligomerization of complexes **5** and **6** upon activation with MAO or MMAO and the results are listed in Table 1. All catalytic reactions shown in Table 1 were carried out at 20 °C and 1 atm ethylene pressure for 0.5 h. When MMAO was used as the co-catalyst, the Al/Ni ratio of 800:1 revealed very low catalytic activity for complexes **5** and **6**. Complex **5** exhibited the highest catalytic activity upon activation with 1000 equiv. of MMAO, while complex **6** reached its best activity in the presence of 1500 equiv. of MMAO (Entries 2 and 6 in Table 1). When MAO was used as the co-catalyst, the Al/Ni ratio of 800:1 gave the best catalytic activities for both complexes **5** and **6** (Entries 1 and 4 in Table 1). Higher or lower Al/Ni ratios resulted in a decline of the catalytic activities. The catalytic reactions predominantly formed dimers of ethylene in the presence of either MAO or MMAO, and the content of α-olefin is from 24.9 to 77.8%.

It was reported that in the catalytic reaction of bis(chelate)nickel complexes the active species was in situ generated by treatment of the nickel complexes with the organoaluminum compound under ethylene.[20c–20e,21] In our catalytic systems, the bis(chelate)nickel complexes **5** and **6** may go through a similar reaction in the presence of MAO and ethylene as shown in Figure 5. Thus, active species **I** was generated by reaction of **5** or **6** with MAO and ethylene. The active intermediate may be stabilized by a weak coordination of the RO group to the nickel center. Subsequently, the ethylene molecule coordinates to the nickel center to carry out the further reactions.

The nickel complexes **9**–**12** can catalyze ethylene dimerization and trimerization in the presence of MAO, MMAO, or Et_2AlCl. However, using Et_2AlCl as the co-catalyst revealed higher activity. Therefore, a systematic investigation of the catalytic behavior of complexes **9**–**12** was performed using Et_2AlCl as the co-catalyst (Table 2). In each case the polymerization reaction gave a mixture of C_4 and C_6 species. At 20 °C and 1 atm ethylene pressure for 0.5 h, the Al/Ni molar ratio of 200:1 afforded the highest catalytic activity for complexes **9**–**12** (**9**, 1.2×10^3; **10**, 1.21×10^3; **11**, 1.82×10^3; and **12**, 1.25×10^3 kg/mol h, respectively, Entries 2, 5, 8, and 17 in Table 2). Longer reaction times resulted in decline of both turnover frequency and the proportion of C_4 components (Entries 15 and 18 in Table 2). The decrease of the activity can be attributed to the deactivation of the active species during a longer reaction period. In the reaction catalyzed by **9**/Et_2AlCl, augmentation of the Al/Ni ratio resulted in enhancement of the proportion of

Table 1. Ethylene oligomerization with complexes **5** and **6**.[a]

Entry	Complex	Co-catalyst	Al/M	Activity[b]	C_4 [%][c]	α-C_4[c]	C_6 [%][c]	α-C_6[c]
1	**5**	MAO	800	78	>99	24.9		
2	**5**	MMAO	1000	395	>99	77.8		
3	**5**	MMAO	1500	177	>99	65.7		
4	**6**	MAO	800	71	97.4	51.5	2.6	35.7
5	**6**	MMAO	1000	52	>99	67.8		
6	**6**	MMAO	1500	224	>99	58.6		

[a] Conditions: 5 μmol of pre-catalyst, 30 mL of toluene, 1 atm ethylene, 0.5 h. [b] kg/mol h. [c] Weight percent determined by GC analysis.

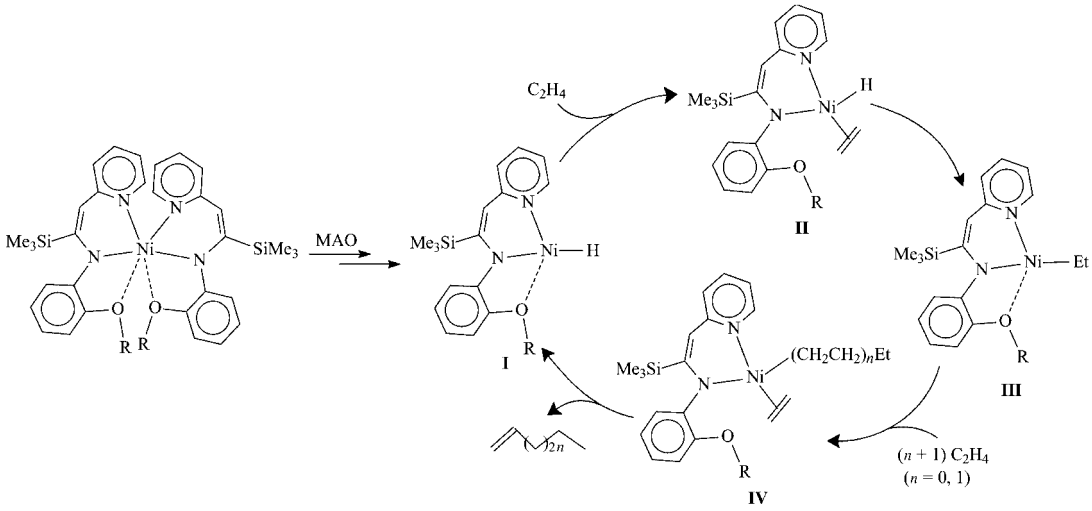

Figure 5. Possible mechanism for ethylene oligomerization catalyzed by **5** and **6**/MAO.

Table 2. Ethylene oligomerization with complexes **9**–**12**.[a]

Entry	Complex	Al/Ni	*P* [atm]	Time [h]	*T* [°C]	Activity[b]	C_4 [%][c]	C_6 [%][c]
1	**9**	50	1	0.5	20	5.4	76.2	23.8
2	**9**	200	1	0.5	20	12	76.4	23.6
3	**9**	400	1	0.5	20	2.45	97.2	2.8
4	**9**	600	1	0.5	20	2.21	95.0	5.0
5	**10**	200	1	0.5	20	12.1	60.2	39.8
6	**11**	50	1	0.5	20	7.78	83.8	16.2
7	**11**	100	1	0.5	20	8.47	86.3	13.7
8	**11**	200	1	0.5	20	18.2	72.3	27.7
9	**11**	300	1	0.5	20	4.83	89.4	10.6
10	**11**	400	1	0.5	20	4.3	91.4	8.6
11	**11**	500	1	0.5	20	2.72	82.0	18.0
12	**11**	200	1	0.5	0	5.65	88.2	11.8
13	**11**	200	1	0.5	40	4.27	59.0	41.0
14	**11**	200	1	0.5	60	3.28	6.7	93.3
15	**11**	200	1	1	20	12.8	46.2	53.8
16	**11**	200	10	0.5	20	92	78.0	22.0
17	**12**	200	1	0.5	20	12.5	66.2	33.8
18	**12**	200	1	1	20	8.72	59.8	40.2
19	**12**	200	10	0.5	20	8.63	75.8	24.2

[a] Conditions: 5 μmol of pre-catalyst, Et_2AlCl as co-catalyst, 30 mL of toluene (120 mL of toluene when determined under 10 atm ethylene). [b] 10^2 kg/mol h. [c] Weight percent determined by GC analysis.

C_4 component in the products. While in the reaction catalyzed by the **11**/Et_2AlCl system, the Al/Ni ratio of 400:1 gave the highest proportion of C_4 component. A change in the reaction temperature also dramatically affected the distribution of the polymerization products. We tested the catalytic reaction of the **11**/Et_2AlCl system with a 200:1 Al/Ni ratio under 1 atm ethylene pressure at 0 °C, 20 °C, 40 °C, and 60 °C, respectively, and found that the proportion of C_6 component increased as the reaction temperature increased (Entries 8 and 12–14 in Table 2). In addition, it was also noted that an increase in ethylene pressure did not enhance the catalytic activity of the catalysts in terms of unit pressure (Entries 16 and 19 in Table 2).

It has been reported that (β-diimine)nickel and (8-quinolylimine)nickel catalysts (Scheme 3) showed very low catalytic activity for ethylene polymerization compared with (α-diimine)nickel complexes and the difference was attributed to the chelate ring size.[6] In our catalytic systems each of the complexes **9**–**12** exhibited good catalytic activity under the optimal conditions. Single-crystal X-ray diffraction results show that complex **12** has a similar skeletal structure and bond lengths and angles to that of the (β-diimine)nickel complex $[CH_2\{C(Me)=NAr\}_2]NiBr_2$ (Ar = 2,6-iPr$_2$C$_6$H$_3$).[6a] Therefore, the relatively high catalytic activity of **9**–**12** is most likely the result of the existence of the *o*-

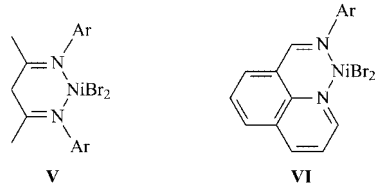

Scheme 3.

OR substituent on the phenylene ring of the ligands. The oxygen atom of the OR group may stabilize the active intermediate through coordination to the metal center during the reaction (see below).

The nature of aluminum co-catalysts greatly affected the catalytic activities of the pre-catalysts and the distribution of the products. The cobalt and iron complexes **13**–**16** were inactive for ethylene oligomerization when Et_2AlCl was used as the co-catalyst. However, these cobalt and iron complexes exhibited catalytic activities for ethylene oligomerization in the presence of MMAO or MAO (Table 3). When MMAO was used as the co-catalyst, the complexes revealed high catalytic activity (up to 8.01×10^2 kg/mol h, Entry 12 in Table 3) and the polymerization products were almost solely C_4 species in most cases. When MAO was used as the co-catalyst, complexes **13** and **14** showed very low catalytic activity, while **15** and **16** exhibited moderate activity (up to 24.6 kg/mol h, Entry 14 in Table 3) and the major polymerization products were C_6 species. We also examined the effect of Al/M ratio for complexes **13** and **15**, respectively. When MMAO was used as co-catalyst, the catalytic activity increased with the enhancement of Al/M molar ratio until 1500:1 for complex **13** and 2000:1 for complex **15** (Entries 4 and 11 in Table 3). When MAO was used as co-catalyst, the Al/Co ratio of 800:1 resulted in the highest catalytic activity for complex **15** (Entry 14 in Table 3), higher or lower Al/Co ratios leading to decrease of the catalytic activity.

Table 3. Ethylene oligomerization with complexes **13**–**16**.[a]

Entry	Complex	Co-catalyst	Al/M	Activity[b]	C_4 [%][c]	C_6 [%][c]
1	**13**	MMAO	500	121	98.4	1.6
2	**13**	MMAO	800	195	98.7	1.3
3	**13**	MMAO	1000	233	98.9	1.1
4	**13**	MMAO	1500	550	92.8	7.2
5	**13**	MMAO	2000	518	99.3	0.7
6	**14**	MMAO	1500	430	99.4	0.6
7	**15**	MMAO	500	174	96.0	4.0
8	**15**	MMAO	800	340	99.3	0.7
9	**15**	MMAO	1000	426	99.4	0.6
10	**15**	MMAO	1500	470	99.5	0.5
11	**15**	MMAO	2000	623	99.8	0.2
12	**16**	MMAO	2000	801	99.6	0.4
13	**15**	MAO	500	8.5	3.0	97.0
14	**15**	MAO	800	24.6	19.8	80.2
15	**15**	MAO	1000	12.8	10.5	89.5
16	**15**	MAO	1200	6	4.9	95.1
17	**16**	MAO	800	11	21.0	79.0

[a] Conditions: 5 μmol of pre-catalyst, 30 mL of toluene, 1 atm ethylene, 20 °C, 0.5 h. [b] kg/mol h. [c] Weight percent determined by GC analysis.

It is very rare to see that iron and cobalt complexes with a six-membered *N*,*N*-chelate ring exhibit high catalytic activity for ethylene polymerization or oligomerization. Good activity shown by complexes **13**–**16** upon activation with MMAO is also attributed to the existence of *o*-OR substituents on the phenylene ring of the ligands.

The proportion of terminal olefins in the dimers or trimers was also determined for the reactions catalyzed by complexes **9**–**16** under representative reaction conditions (Table 4). At 20 °C and 1 atm ethylene pressure for 0.5 h, the reactions catalyzed by the **9**–**12**/Et_2AlCl (1:200) systems gave relatively low α-butene and α-hexene proportions. When activated with MMAO, each of the complexes **13**–**16** led to relatively high α-butene proportions, from 84.5 to 90.7%.

In order to understand the role of *o*-OR substituents on the phenylene ring of the ligands in complexes **9**–**16**, we investigated the catalytic behavior of complex **18** whose ligand does not contain an extra donor group on the phenylene ring. The results are shown in Table 5. Compared with complexes **11** and **12** under the same polymerization conditions, complex **18** exhibited lower catalytic activity. Hence, we think that the existence of *o*-RO substituents on the phenylene ring in the nickel complexes may stabilize the active intermediate through a weak coordination of the oxygen atom to the metal center, which leads to the rise in their catalytic activities (Scheme 4). Although the stabilizing action of the aluminum activator to the active intermediate is usually important, the intramolecular coordination may provide extra stabilization in our catalytic systems. Bianchini and co-workers also observed that complex **IX** exhibits higher catalytic activity than complex **X** in ethylene oligomerization upon activation with MAO and they thought that the sulfur atom of the former may play an active role (Scheme 5).[22] In addition, the activity of complex **19** is also lower than that of complexes **15** or **16** whether MAO or MMAO was used as the co-catalyst. This is possibly due to the existence of the same stabilization in the **15** or **16**/activator system.

Table 4. Oligomer composition catalyzed by pre-catalysts **9**–**16**[a].

Entry	Complex	Co-catalyst	Al/Ni	*T* [°C]	Activity[b]	C_4 [%][c]	α-C_4 [%][c]	C_6 [%][c]	α-C_6 [%][c]
1	**9**	Et_2AlCl	200	20	10.8	79.8	26.4	20.2	32.4
2	**10**	Et_2AlCl	200	20	11.2	66.0	18.6	34	29.5
3	**11**	Et_2AlCl	200	20	17.1	78.0	29.7	22.0	44.3
4	**11**	Et_2AlCl	200	0	5.77	85.6	36.6	14.4	38.2
5	**12**	Et_2AlCl	200	20	11.5	69.4	32.0	30.6	26.4
6	**13**	MMAO	1500	20	5.75	97.7	90.7	2.3	28
7	**14**	MMAO	1500	20	4.14	>99	86.4		
8	**15**	MMAO	2000	20	6.72	>99	84.5		
9	**16**	MMAO	2000	20	8.28	>99	90.0		

[a] Conditions: 5 μmol of pre-catalyst, 30 mL of toluene, 1 atm ethylene, 0.5 h. [b] 10^2 kg/mol h. [c] Weight percent determined by GC analysis.

Table 5. Ethylene oligomerization with complexes **18** and **19**.[a]

Entry	Complex	Co-catalyst	Al/M	Activity[b]	C_4 [%][c]	α-C_4 [%][c]	C_6 [%][c]	α-C_6 [%][c]
1	**18**	Et_2AlCl	100	126	43.8	11.6	56.2	23.7
2	**18**	Et_2AlCl	200	159	98.2	58.5	1.8	14.5
3	**18**	Et_2AlCl	500	220	45.5	29.5	54.5	12.3
4	**19**	MMAO	800	142	98.4	65.7	1.6	56.4
5	**19**	MMAO	2000	129	>99	98		
6	**19**	MAO	800	4	81.6		18.4	
7	**19**	MAO	2000	1.2	37.8		62.2	

[a] Conditions: 5 μmol of pre-catalyst, 30 mL of toluene, 1 atm ethylene, 0.5 h. [b] kg/mol h. [c] Weight percent determined by GC analysis.

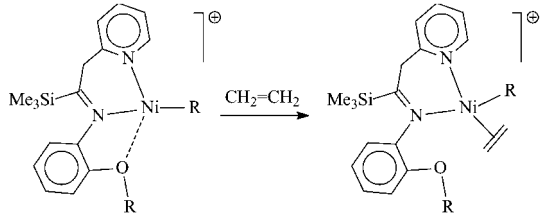

Scheme 4. Possible active intermediates of **9**–**12**/Et_2AlCl systems.

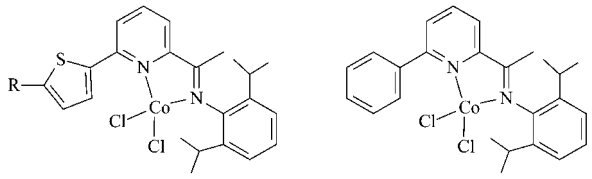

Scheme 5.

Conclusions

We have synthesized novel anionic and neutral *N*,*N*-chelate ligands and their iron, cobalt, and nickel complexes. Single-crystal X-ray diffraction revealed that in bis(chelate)-nickel complex **6** there are relatively weak bonding interactions between the O atoms and the Ni atoms. Investigation of catalytic behavior for ethylene oligomerization showed that complexes **5** and **6** could catalyze ethylene oligomerization with good activity in the presence of MAO or MMAO, giving mainly C_4 species. The nickel complexes with neutral ligands exhibited high catalytic activity upon activation with Et_2AlCl. This relatively high activity compared with previously reported (β-diimine)nickel complexes and analogues is attributed to the stabilizing action of the *o*-OR group on the phenylene ring of the ligands to the active species through coordination of the oxygen atom to the metal center. The iron and cobalt complexes bearing neutral ligands also exhibited good catalytic activity upon activation with MMAO. However, when MAO was used as the co-catalyst, the iron and cobalt complexes showed relatively low activities.

Experimental Section

General Procedure: All air-sensitive manipulations were performed under N_2 using standard Schlenk and vacuum-line techniques. Solvents were distilled under N_2 from sodium/benzophenone (toluene, *n*-hexane, thf, and Et_2O) or CaH_2 (CH_2Cl_2) and degassed prior to use. NMR spectra were recorded with a Bruker av300 spectrometer at ambient temperature. The chemical shifts of ^1H and ^{13}C NMR spectra are referenced to internal solvent resonances. IR spectra were recorded with a Bruker VECTOR-22 spectrometer. HRMS data were determined with an Agilent6890/Micromass GCT-MS spectrometer. Elemental analyses were performed by the Analytical Center of the University of Science and Technology of China. The magnetic moments of the paramagnetic complexes were determined by the Evans NMR method.[23] Gas chromatographic analyses were performed with a Carlo Erba Strumentazione gas chromatograph equipped with a flame-ionization detector and a 30 m (0.25 mm i.d., 0.25-μm film thickness) DM-1 silica capillary column or with an HP5890 gas chromatograph equipped with a flame-ionization detector and a 30 m (0.25 mm i.d., 0.25-μm film thickness) CAT-7221 silica capillary column. High-purity ethylene was purchased from Beijing Yanshan Petrochemical Co. and used as received. Methylaluminoxane (MAO, 1.46 M in toluene) and modified methylaluminoxane (MMAO, 1.93 M in heptane) were purchased from Akzo Nobel Corp. Et_2AlCl was purchased from Fluka as a 1.90 M solution in hexane.

Preparations

***o*-PhCH$_2$OC$_6$H$_4$NC (1):** Compound **1** was prepared according to a literature method.[12] ^1H NMR ($CDCl_3$): δ = 5.20 (s, 2 H, CH_2), 6.91–7.01 (m, 2 H, Ph, C_6H_4), 7.26–7.49 (m, 7 H, Ph, C_6H_4) ppm. IR (KBr): $\tilde{\nu}$ = 3072 (w), 3034 (w), 2947 (w), 2936 (w), 2876 (w), 2127 (vs), 1593 (s), 1492 (vs), 1469 (m), 1454 (s), 1382 (m), 1301 (m), 1287 (vs), 1251 (vs), 1162 (m), 1109 (s), 1080 (w), 1040 (w), 1001 (s), 932 (w), 917 (m), 857 (m), 760 (m), 744 (vs), 695 (s), 617 (w) cm^{-1}.

***o*-*i*PrOC$_6$H$_4$NC (2):** Compound **2** was prepared according to the same method as for **1** as a colorless oil, b.p. 100 °C/2 Torr. ^1H NMR ($CDCl_3$): δ = 1.33 (d, J = 6.1 Hz, 6 H, *i*Pr), 4.55 (sept, J = 6 Hz, 1 H, CH), 6.80–6.91 (m, 2 H, C_6H_4), 7.21–7.27 (m, 2 H, C_6H_4) ppm. IR (liquid film): $\tilde{\nu}$ = 3076 (w), 2981 (s), 2935 (m), 2125 (vs), 1596 (s), 1492 (vs), 1455 (m), 1386 (m), 1376 (m), 1286 (s), 1260 (s), 1176 (w), 1162 (m), 1139 (m), 1117 (s), 1043 (m), 952 (s), 867 (w), 752 (s) cm^{-1}.

[LiN(*o*-PhCH$_2$OC$_6$H$_4$){C(SiMe$_3$)CHC$_5$H$_4$N-2}]$_2$ (3): To a stirred solution of [Li(TMEDA){2-CH(SiMe$_3$)C$_5$H$_4$N}] (3.84 g, 13.38 mmol) in diethyl ether (20 mL) was added compound **1** (2.80 g, 13.40 mmol) at –30 °C. The resultant solution was warmed to room temperature and stirred overnight. The mixture was filtered and the precipitate was washed with diethyl ether (2 × 5 mL). The solid was dried in vacuo to give a yellow powder of **3** (4.21 g, 82.7%), m.p. 181–182 °C. ^1H NMR (C_6D_6): δ = 0.48 (s, 9 H, $SiMe_3$), 4.42 (d, J = 11.7 Hz, 1 H, CH_2), 4.58 (d, J = 11.4 Hz, 1 H, CH_2), 5.62 (s, 1 H, CH), 6.48–6.53 (m, 1 H, Ar), 6.57 (d, J = 8.4 Hz, 1 H, Ar), 6.66 (d, J = 7.8 Hz, 1 H, Ar), 6.92–7.22 (m, 6 H,

Ar), 7.42 (d, J = 7.8 Hz, 1 H, Ar), 7.98–8.01 (m, 1 H, Ar) ppm. ^{13}C NMR (C_6D_6): δ = 2.60, 70.17, 110.49, 110.88, 114.93, 119.02, 121.95, 122.38, 125.24, 128.22, 128.57, 128.81, 135.52, 136.35, 147.24, 148.87, 151.64, 157.50, 168.08 ppm. $C_{23}H_{25}LiN_2OSi$ (380.484): calcd. C 72.60, H 6.62, N 7.36; found C 71.92, H 6.62, N 7.30.

[LiN(*o*-*i*PrOC$_6$H$_4$){C(SiMe$_3$)CHC$_5$H$_4$N-2}]$_2$ (4): Complex **4** was prepared according to the same method as for **3**. To a solution of [Li(TMEDA){2-CH(SiMe$_3$)C$_5$H$_4$N}] (3.55 g, 12.37 mmol) in diethyl ether (20 mL) was added compound **2** (2.00 g, 12.42 mmol) at –30 °C. The mixture was warmed to room temperature and stirred overnight. The resultant precipitate was washed with diethyl ether and dried in vacuo to afford a yellow powder of **4** (3.85 g, 93.5%), m.p. 242–243 °C. ^{1}H NMR (C_6D_6): δ = 0.46 (s, 9 H, SiMe$_3$), 0.97 (d, J = 6 Hz, 3 H, *i*Pr), 1.35 (d, J = 6 Hz, 3 H, *i*Pr), 4.36 (heptet, J = 6 Hz, 1 H, *i*Pr), 5.81 (s, 1 H, CH), 6.68–6.75 (m, 2 H, Ar), 6.84 (d, J = 8.4 Hz, 1 H, Ar), 7.01–7.06 (m, 1 H, Ar), 7.14–7.17 (m, 2 H, Ar), 7.21–7.27 (m, 1 H, Ar), 8.40 (dd, J = 1.2, 5.1 Hz, 1 H, Ar) ppm. ^{13}C NMR (C_6D_6): δ = 2.40, 20.43, 22.01, 70.29, 110.85, 110.93, 115.39, 119.21, 121.71, 123.20, 125.70, 135.86, 147.17, 149.42, 150.43, 157.97, 169.99 ppm. $C_{19}H_{25}LiN_2OSi$ (332.441): calcd. C 68.64, H 7.58, N 8.43; found C 68.21, H 7.57, N 8.26.

Ni[N(*o*-PhCH$_2$OC$_6$H$_4$){C(SiMe$_3$)CHC$_5$H$_4$N-2}]$_2$ (5): To a stirred suspension of (dme)NiCl$_2$ (0.15 g, 0.684 mmol) in thf (5 mL) was added compound **3** (0.26 g, 0.684 mmol) at about –80 °C. The resultant mixture was warmed to room temperature and stirred overnight. Volatiles were removed in vacuo and the residue was extracted with Et$_2$O. The diethyl ether solution was filtered and the filtrate concentrated in vacuo to form dark red-brown crystals of **5** (0.25 g, 91%), m.p. 169–170 °C. IR (KBr): $\tilde{\nu}$ = 3088 (vw), 3053 (w), 3024 (w), 2951 (w), 2894 (vw), 1600 (m), 1572 (w), 1557 (w), 1501 (m), 1481 (s), 1469 (vs), 1453 (m), 1418 (m), 1384 (vs), 1314 (w), 1277 (m), 1260 (m), 1246 (m), 1208 (m), 1189 (m), 1153 (m), 1113 (w), 1102 (vw), 1022 (w), 1004 (w), 847 (m), 783 (w), 751 (w), 732 (m), 693 (w) cm^{-1}. $C_{46}H_{50}N_4NiO_2Si_2$ (805.779): calcd. C 68.57, H 6.25, N 6.95; found C 68.77, H 6.43, N 6.90. HRMS (EI): calcd. for $C_{46}H_{50}N_4NiO_2Si_2$ [M]$^+$ 804.2826; found 804.2820. μ_{eff} = 3.77 BM.

Ni[N(*o*-*i*PrOC$_6$H$_4$){C(SiMe$_3$)CHC$_5$H$_4$N-2}]$_2$ (6): Complex **6** was prepared according to a procedure similar to that of **5**. Reaction of (dme)NiCl$_2$ (0.195 g, 0.886 mmol) with **4** (0.30 g, 0.904 mmol) in thf gave, after workup, dark red-brown crystals of **6** (0.295 g, 92%), m.p. 180–182 °C. IR (KBr): $\tilde{\nu}$ = 3052 (vw), 2974 (w), 2948 (w), 2894 (w), 1599 (m), 1572 (w), 1558 (w), 1503 (m), 1480, 1469 (vs), 1420 (s), 1369 (vs), 1309 (w), 1289 (s), 1265 (s), 1244 (m), 1207 (m), 1154 (m), 1138 (m), 1117 (m), 1048 (w), 1005 (w), 948 (w), 846 (s), 786 (s), 740 (s), 684 (vw), 621 (vw) cm^{-1}. $C_{38}H_{50}N_4NiO_2Si_2$ (709.694): calcd. C 64.31, H 7.10, N 7.89; found C 64.39, H 7.03, N 8.01. HRMS (EI): calcd. for $C_{38}H_{50}N_4NiO_2Si_2$ [M]$^+$ 708.2826; found 708.2823. μ_{eff} = 3.70 BM.

***o*-PhCH$_2$OC$_6$H$_4$NHC(SiMe$_3$)CHC$_5$H$_4$N-2 (7):** To a stirred solution of **3** (1.488 g, 3.92 mmol) in toluene (20 mL) was added Et$_3$NH$^+$Cl$^-$ (0.54 g, 3.93 mmol) at 0 °C. The resultant mixture was warmed to room temperature and stirred for 20 h. The solution was filtered and volatiles were removed from the filtrate in vacuo to afford **7** as a yellowish oil (1.464 g, 100%). The oil was dissolved in hexane and cooled to –30 °C to form a pale yellow precipitate. The precipitate was filtered at –30 °C and then dried in vacuo to afford a pale yellow solid, m.p. 81–83 °C. ^{1}H NMR ($CDCl_3$): δ = 0.20 (s, 9 H, SiMe$_3$), 5.17 (s, 2 H, CH$_2$), 5.69 (s, 1 H, CH), 6.84–6.95 (m, 4 H, Ar), 7.02 (d, J = 8.1 Hz, 1 H, Ar), 7.10 (d, J = 7.5 Hz, 1 H, Ar), 7.29–7.37 (m, 3 H, Ar), 7.48–7.55 (m, 3 H, Ar), 8.23–8.25 (m, 1 H, Ar), 11.77 (s, 1 H, NH) ppm. ^{13}C NMR ($CDCl_3$): δ = 1.01, 70.29, 109.88, 112.66, 118.26, 120.78, 122.16, 122.32, 122.65, 127.22, 127.72, 128.53, 134.31, 135.63, 137.55, 147.37, 150.62, 152.84, 159.30 ppm. IR (liquid film): $\tilde{\nu}$ = 3064 (w), 3036 (w), 2953 (w), 2897 (vw), 1590 (s), 1577 (vs), 1540 (vs), 1507 (m), 1463 (m), 1450 (m), 1411 (w), 1360 (m), 1301 (w), 1259 (s), 1217 (s), 1158 (w), 1109 (w), 1046, 1024 (w), 911 (vw), 847 (s), 804 (m), 738 (s), 694 (m) cm^{-1}. $C_{23}H_{26}N_2OSi$ (374.551): calcd. C 73.76, H 7.00, N 7.48; found C 73.46, H 7.10, N 7.40.

***o*-*i*PrOC$_6$H$_4$NHC(SiMe$_3$)CHC$_5$H$_4$N-2 (8):** Compound **8** was prepared according to a procedure similar to that of **7**. Treatment of **4** (1.412 g, 4.25 mmol) with Et$_3$NH$^+$Cl$^-$ (0.60 g, 4.36 mmol) in toluene afforded, after workup, compound **8** (1.386 g, 100%) as a yellowish oil. ^{1}H NMR ($CDCl_3$): δ = 0.13 (s, 9 H, SiMe$_3$), 1.31 (d, J = 6 Hz, 6 H, *i*Pr), 4.47 (sept, J = 6 Hz, 1 H, *i*Pr), 5.59 (s, 1 H, CH), 6.74–6.85 (m, 4 H, Ar), 6.92–6.98 (m, 2 H, Ar), 7.40–7.46 (m, 1 H, Ar), 8.32–8.34 (m, 1 H, Ar), 11.58 (s, 1, NH) ppm. ^{13}C NMR ($CDCl_3$): δ = 1.04, 22.39, 71.36, 109.77, 115.16, 118.19, 120.66, 121.50, 122.22, 122.26, 135.33, 135.58, 147.19, 149.33, 152.39, 159.22 ppm. IR (liquid film): $\tilde{\nu}$ = 3065 (w), 3007 (w), 2975 (m), 2904 (w), 1590 (vs), 1578 (vs), 1540 (vs), 1505 (m), 1463 (m), 1411 (w), 1361 (m), 1301 (w), 1258 (vs), 1218 (s), 1160 (w), 1150 (w), 1118 (m), 1044 (vw), 956 (vw), 912 (vw), 848 (s), 802 (m), 739 (m), 687 (w) cm^{-1}. $C_{19}H_{26}N_2OSi$ (326.508): calcd. C 69.89, H 8.03, N 8.58; found C 69.72, H 8.13, N 8.46.

[NiCl$_2${N(*o*-PhCH$_2$OC$_6$H$_4$)=C(SiMe$_3$)CH$_2$C$_5$H$_4$N-2}] (9): To a stirred suspension of (dme)NiCl$_2$ (0.35 g, 1.59 mmol) in thf (5 mL) was added **7** (0.60 g, 1.60 mmol) in thf (10 mL) at 0 °C. The mixture was warmed to room temperature and stirred overnight. Volatiles were removed in vacuo and the yellow solids were washed with Et$_2$O (2 × 2 mL). The solid was dissolved in CH_2Cl_2 and filtered through Celite. Toluene (10 mL) was added to the filtrate. Concentration of the solution in vacuo gave yellow-green crystals of complex **9** (0.59 g, 74.2%), m.p. 192–194 °C. IR (KBr): $\tilde{\nu}$ = 3057 (s), 3036 (m), 2951 (m), 2897 (vw), 2875 (m), 1603 (s), 1590 (m), 1579 (m), 1488 (vs), 1452 (s), 1442 (s), 1397 (w), 1377 (w), 1347 (w), 1320 (m), 1288 (m), 1267 (m), 1254 (s), 1235 (s), 1207 (m), 1195 (m), 1161 (m), 1115 (m), 1063 (m), 1045 (m), 1018 (s), 897 (w), 871 (s), 846 (vs), 791 (w), 758 (vs), 736 (s), 725 (s), 692 (m), 651 (w), 634 (w) cm^{-1}. $C_{23}H_{26}Cl_2N_2NiOSi$ (504.15): calcd. C 54.80, H 5.20, N5.56; found C 55.01, H 5.27, N 5.45. HRMS (EI): calcd. for $C_{23}H_{26}ClN_2NiOSi$ [M – Cl]$^+$ 467.0856; found 467.1482. μ_{eff} = 3.82 BM.

[NiCl$_2${N(*o*-*i*PrOC$_6$H$_4$)=C(SiMe$_3$)CH$_2$C$_5$H$_4$N-2}] (10): Complex **10** was prepared according to a procedure similar to that for **9**. Treatment of (dme)NiCl$_2$ (0.27 g, 1.23 mmol) with **8** (0.40 g, 1.23 mmol) in thf formed, after similar workup, purple crystals of **10** (0.42 g, 75.1%), m.p. 182–184 °C. IR (KBr): $\tilde{\nu}$ = 3104 (vw), 3068 (w), 3029 (w), 2977 (m), 2931 (w), 2896 (w), 1605 (m), 1592 (s), 1569 (w), 1485 (vs), 1446 (s), 1417 (w), 1372 (w), 1358 (w), 1283 (vw), 1250 (s), 1203 (w), 1176 (w), 1159 (w), 1139 (w), 1120 (w), 1095 (m), 1067 (w), 1030 (w), 955 (w), 933 (w), 924 (w), 853 (vs), 803 (w), 765 (vs), 700 (w), 680 (vw) cm^{-1}. $C_{19}H_{26}Cl_2N_2NiOSi$ (456.107): calcd. C 50.03, H 5.75, N 6.14; found C 49.93, H 5.74, N 6.14. HRMS (EI): calcd. for $C_{19}H_{26}ClN_2NiOSi$ [M – Cl]$^+$ 419.0856; found 419.0849. μ_{eff} = 3.88 BM.

[NiBr$_2${N(*o*-PhCH$_2$OC$_6$H$_4$)=C(SiMe$_3$)CH$_2$C$_5$H$_4$N-2}] (11): To a stirred suspension of NiBr$_2$ (0.14 g, 0.64 mmol) in thf (5 mL) was added **7** (0.25 g 0.67 mmol) in thf (10 mL) at 0 °C. The resultant mixture was warmed to room temperature and stirred overnight. The color of the solution changed from straw-yellow to red. Volatiles were removed in vacuo and the red solid residue was dissolved in CH_2Cl_2. After filtration through Celite, the solvent was removed

from the filtrate and the solid was washed with diethyl ether (2 × 2 mL) to give red crystalline **11** (0.302 g, 77.4%), m.p. 189–191 °C. IR (KBr): ṽ = 3056 (m), 2953 (m), 2860 (m), 1604 (m), 1593 (m), 1574 (w), 1486 (s), 1444 (s), 1407 (w), 1372 (w), 1348 (w), 1315 (w), 1285 (w), 1253 (s), 1239 (m), 1205 (w), 1161 (w), 1112 (m), 1067 (w), 1040 (w), 1020 (m), 942 (vw), 921 (vw), 904 (vw), 851 (vs), 801 (w), 766 (s), 735 (s), 695 (m), 655 (vw), 632 (w), 613 (vw) cm^{-1}. $C_{23}H_{26}Br_2N_2NiOSi$ (593.052): calcd. C 46.58, H 4.42, N 4.72; found C 46.66, H 4.39, N 4.70. HRMS (EI): calcd. for $C_{23}H_{26}Br_2N_2NiOSi$ $[M]^+$ 589.9535; found 589.9540. μ_{eff} = 3.86 BM.

[NiBr$_2${N(*o*-*i*PrOC$_6$H$_4$)=C(SiMe$_3$)CH$_2$C$_5$H$_4$N-2}] (12): Complex **12** was prepared according to the same route as for **11**. Thus, reaction of $NiBr_2$ (0.15 g, 0.68 mmol) with **8** (0.23 g, 0.70 mmol) in thf gave, after similar workup, complex **12** (0.30 g, 78.9%) as red crystals, m.p. 209–211 °C. IR (KBr): ṽ = 3103 (w), 3070 (w), 3028 (w), 2974 (m), 2934 (w), 2903 (w), 1595 (s), 1569 (vw), 1488 (vs), 1445 (s), 1422 (w), 1384 (m), 1375 (m), 1351 (w), 1301 (m), 1280 (m), 1252 (vs), 1207 (w), 1174 (w), 1158 (w), 1141 (w), 1118 (s), 1071 (vw), 1039 (w), 1031 (w), 956 (m), 846 (vs), 772 (s), 758 (s), 705 (vw), 677 (vw), 643 (w) cm^{-1}. $C_{19}H_{26}Br_2N_2NiOSi$ (545.01): calcd. C 41.87, H 4.81, N 5.14; found C 41.97, H 4.80, N 5.16. HRMS (EI): calcd. for $C_{19}H_{26}Br_2N_2NiOSi$ $[M]^+$ 541.9535; found 541.9536. μ_{eff} = 4.20 BM.

[FeCl$_2${N(*o*-PhCH$_2$OC$_6$H$_4$)=C(SiMe$_3$)CH$_2$C$_5$H$_4$N-2}] (13): Complex **13** was prepared according to a procedure similar to that for **11**. Treatment of $FeCl_2{\cdot}4H_2O$ (0.188 g, 0.945 mmol) with **7** (0.358 g, 0.957 mmol) in thf afforded, after similar workup, a yellow crystalline complex (0.3 g, 63%) as yellow crystals, m.p.189–191 °C. IR (KBr): ṽ = 3065 (m), 3030 (m), 2956 (m), 1593 (s), 1569 (w), 1491 (s), 1484 (m), 1445 (s), 1381 (w), 1344 (w), 1280 (w), 1253 (vs), 1203 (w), 1162 (w), 1115 (m), 1063 (w), 1022 (m), 850 (vs), 809 (w), 773 (s), 761 (vs), 730 (m), 692 (m), 675 (w), 639 (w), 615 (w) cm^{-1}. $C_{23}H_{26}Cl_2FeN_2OSi$ (501.301): calcd. C 55.11, H 5.23, N 5.59; found C 54.89, H 5.10, N 5.54. HRMS (EI): calcd. for $C_{23}H_{26}Cl_2FeN_2OSi$ $[M]^+$ 500.0541; found 500.0550. μ_{eff} = 7.00 BM.

[FeCl$_2${N(*o*-*i*PrOC$_6$H$_4$)=C(SiMe$_3$)CH$_2$C$_5$H$_4$N-2}] (14): Complex **14** was prepared according to a procedure similar to that for **11**. Treatment of $FeCl_2{\cdot}4H_2O$ (0.191 g, 0.96 mmol) with **8** (0.302 g, 0.926 mmol) in thf formed, after similar workup, yellow crystalline complex **14** (0.296 g, 71.4%) as yellow crystals, m.p.178–180 °C. IR (KBr): ṽ = 3102 (m), 3067 (m), 3027 (m), 2979 (s), 2899 (m), 1604 (m), 1585 (m), 1568 (w), 1484 (vs), 1444 (s), 1382 (w), 1374 (w), 1348 (w), 1279 (w), 1249 (s), 1201 (w), 1157 (w), 1141 (w), 1118 (m), 1063 (w), 1037 (w), 1022 (w), 953 (w), 934 (w), 854 (vs), 772 (s), 730 (m), 696 (w), 676 (vw), 640 (w), 607 (w) cm^{-1}. $C_{19}H_{26}Cl_2FeN_2OSi$ (453.259): calcd. C 50.35, H 5.78, N 6.18; found C 50.29, H 5.70, N 6.08. HRMS (EI): calcd. for $C_{19}H_{26}Cl_2FeN_2OSi$ $[M]^+$ 452.0541; found 452.0527. μ_{eff} = 6.93 BM.

[CoCl$_2${N(*o*-PhCH$_2$OC$_6$H$_4$)=C(SiMe$_3$)CH$_2$C$_5$H$_4$N-2}] (15): To a solution of $CoCl_2$ (0.067 g, 0.515 mmol) in thf (5 mL) was added **7** (0.196 g, 0.524 mmol) in thf (10 mL) at 0 °C while stirring. The mixture was warmed to room temperature and stirred overnight. The color of the solution changed to blue. Volatiles were removed in vacuo and the residue was washed with diethyl ether (2 × 2 mL). The solid was dissolved in CH_2Cl_2 and then filtered. Toluene was added to the solution and then concentrated to afford **15** (0.16 g, 60.8%) as blue crystals, m.p. 196–198 °C. IR (KBr): ṽ = 3072 (w), 3028 (m), 2953 (m), 2897 (w), 1596 (s), 1568 (w), 1492 (s), 1446 (s), 1381 (w), 1347 (w), 1279 (w), 1254 (vs), 1205 (w), 1163 (w), 1116 (w), 1067 (vw), 1039 (w), 1026 (m), 933 (vw), 850 (vs), 774 (s), 763 (vs), 730 (w), 692 (w), 643 (vw) cm^{-1}. $C_{23}H_{26}Cl_2CoN_2OSi$ (504.39): calcd. C 54.77, H 5.20, N 5.55; found C 54.99, H 5.28, N 5.65. HRMS (EI): calcd. for $C_{23}H_{26}Cl_2CoN_2OSi$ $[M]^+$ 503.0523; found 503.0515. μ_{eff} = 6.46 BM.

[CoCl$_2${N(*o*-*i*PrOC$_6$H$_4$)=C(SiMe$_3$)CH$_2$C$_5$H$_4$N-2}] (16): Complex **16** was prepared according to a procedure similar to that for **15**. Treatment of $CoCl_2$ (0.208 g, 1.6 mmol) with **8** (0.532 g, 1.63 mmol) in thf afforded, after workup, complex **16** (0.72 g, 99%) as blue crystals, m.p. 199–201 °C. IR (KBr): ṽ = 3072 (w), 3027 (m), 2978 (m), 2941 (w), 2897 (w), 1605 (m), 1592 (s), 1572 (w), 1488 (vs), 1445 (s), 1379 (m), 1346 (w), 1300 (w), 1280 (w), 1250 (vs), 1207 (w), 1175 (w), 1158 (w), 1142 (w), 1118 (s), 1067 (vw), 1039 (w), 1028 (w), 956 (m), 937 (w), 845 (vs), 774 (s), 760 (vs), 736 (w), 651 (w), 643 (w) cm^{-1}. $C_{19}H_{26}Cl_2CoN_2OSi$ (456.347): calcd. C 50.01, H 5.74, N 6.14; found C 49.99, H 5.58, N 6.13. HRMS (EI): calcd. for $C_{19}H_{26}Cl_2CoN_2OSi$ $[M]^+$ 455.0523; found 455.0523. μ_{eff} = 6.54 BM.

***o*-MeC$_6$H$_4$NHC(SiMe$_3$)CHC$_5$H$_4$N-2 (17):** To a solution of [Li(TMEDA)][2-CH(SiMe$_3$)C$_5$H$_4$N] (1.07 g, 3.73 mmol) in diethyl ether (15 mL) was added 2-methylphenyl isocyanide (0.44 g 3.76 mmol) at –30 °C. The resultant mixture was warmed to room temperature and stirred overnight to give a dark red solution. Volatiles were removed in vacuo and thf (10 mL) was added. To the solution H_2O (0.068 g) was added at 0 °C and the mixture stirred for 10 min to give a greenish-yellow solution. The solvent was removed in vacuo and *n*-hexane was added. The mixture was filtered and the solvent was removed from the filtrate in vacuo. The residue was distilled under reduced pressure to give a pale yellow oil (0.80 g, 76%) as a mixture of (*Z*) and (*E*) isomers [(*Z*)/(*E*) = 1:3.4], b.p. 130 °C/0.1 Torr. ^{1}H NMR (C_6D_6, 300 MHz): (*E*) isomer: δ = 0.24 (s, 9 H, $SiMe_3$), 2.51 (s, 3 H, Me), 5.75 (s, 1 H, =CH), 6.55 (d, J = 9.9 Hz, 1 H, C_6H_4), 6.99–7.33 (m, 5 H, C_6H_4, C_5H_4N), 7.62–7.68 (m, 1 H, C_5H_4N), 8.49–8.51 (m, 1 H, C_5H_4N), 11.76 (s, 1 H, NH) ppm. (*Z*) isomer: δ = 0.34 (s, 9 H, $SiMe_3$), 2.16 (s, 3 H, Me), 5.52 (d, J = 10.2 Hz, 1 H, =CH) ppm, aromatic ring region overlaps that of (*E*) isomer. IR (liquid film): ṽ = 3006 (w), 2953 (m), 2897 (w), 1643 (m), 1622 (s), 1584 (vs), 1539 (s), 1496 (m), 1469 (s), 1410 (m), 1352 (s), 1303 (m), 1250 (s), 1217 (s), 1149 (s), 1110 (w), 1076 (w), 1045 (w), 993 (w), 934 (vw), 912 (w), 848 (vs), 801 (m), 758 (s), 729 (m) cm^{-1}. HRMS (EI): calcd. for $C_{17}H_{22}N_2Si$ $[M]^+$ 282.1552; found 282.1546.

[NiBr$_2${N(*o*-MeC$_6$H$_4$)=C(SiMe$_3$)CH$_2$C$_5$H$_4$N-2}] (18): To a suspension of $NiBr_2$ (0.195 g, 0.89 mmol) in thf (5 mL) was added a solution of **17** (0.25 g 0.89 mmol) in thf (10 mL) at 0 °C. The resultant mixture was warmed to room temperature and stirred overnight. Volatiles were removed in vacuo and the residual solid was dissolved in CH_2Cl_2 and filtered. The solvent was removed in vacuo from the filtrate and the residue washed with thf (3 × 2 mL) to afford purple-red crystals of **18** (0.27 g, 61%), m.p. 274–276 °C. IR (KBr): ṽ = 3102 (w), 3047 (w), 2956 (w), 2917 (w), 1599 (s), 1567 (w), 1482 (s), 1443 (s), 1411 (m), 1359 (w), 1286 (w), 1254 (s), 1191 (w), 1113 (m), 1070 (w), 1041 (w), 1029 (w), 849 (vs), 796 (w), 766 (vs), 718 (w), 703 (w) cm^{-1}. $C_{17}H_{22}Br_2N_2NiSi$ (500.957): calcd. C 40.76, H 4.43, N 5.59; found C 40.87, H 4.49, N 5.78. HRMS (EI): calcd. for $C_{17}H_{22}Br_2N_2NiSi$ $[M]^+$ 497.9272; found 497.9263. μ_{eff} = 3.95 BM.

[CoCl$_2${N(*o*-MeC$_6$H$_4$)=C(SiMe$_3$)CH$_2$C$_5$H$_4$N-2}] (19): To a suspension of $CoCl_2$ (0.092 g, 0.71 mmol) in thf (5 mL) was added a solution of **17** (0.2 g 0.71 mmol) in thf (10 mL) at 0 °C. The resultant mixture was warmed to room temperature and stirred overnight. Volatiles were removed in vacuo and the residue was dissolved in CH_2Cl_2 and filtered. The solvent was removed in vacuo from the filtrate and the residue washed with thf (2 mL × 3) to give a blue

Table 6. Details of the X-ray structure determinations of compounds **3**, **6**, **12**, and **14**.

	3	**6**	**12**	**14**
Empirical formula	$C_{46}H_{50}Li_2N_4O_2Si_2$	$C_{38}H_{50}N_4NiO_2Si_2$	$C_{19}H_{26}Br_2N_2NiOSi$	$C_{19}H_{26}Cl_2FeN_2OSi$
Formula mass	760.96	709.71	545.04	453.26
Crystal system	monoclinic	monoclinic	monoclinic	monoclinic
Space group	$P2_1/c$	$P2_1/n$	$P2(1)/c$	$P2(1)/c$
a [Å]	11.1979(19)	19.736(3)	9.1529(9)	9.1215(12)
b [Å]	23.748(4)	11.1103(15)	10.9906(11)	10.8936(16)
c [Å]	17.346(3)	19.857(3)	23.504(2)	23.224(3)
β [°]	107.884(3)	116.108(2)	95.151(2)	94.339(2)
V [Å^3]	4389.9(13)	3909.8(9)	2354.9(4)	2301.1(5)
Z	4	4	4	4
$D_{calcd.}$ [g/cm^3]	1.151	1.206	1.537	1.308
$F(000)$	1616	1512	1096	944
μ [mm^{-1}]	0.121	0.594	4.278	0.950
θ range for data collection [°]	1.50 to 25.00	1.94 to 26.39	1.74 to 26.46	2.07 to 26.40
No. of reflections collected	18479	21552	12793	12689
No. of independent reflections (R_{int})	7713 (R_{int} = 0.0942)	7978 (R_{int} = 0.0771)	4847 (R_{int} = 0.0336)	4711 (R_{int} = 0.0355)
No. of data/restraints/parameters	7713/0/511	7978/0/434	4847/6/240	4711/6/240
Goodness of fit on F^2	0.995	0.988	0.997	1.004
Final R indices[a] [$I > 2\sigma(I)$]	$R1$ = 0.0673; wR_2 = 0.1324	R_1 = 0.0542; wR_2 = 0.1290	R_1 = 0.0377; wR_2 = 0.0758	R_1 = 0.0409; wR_2 = 0.0876
R indices (all data)	R_1 = 0.1926; wR_2 = 0.1842	R_1 = 0.1481; wR_2 = 0.1688	R_1 = 0.0764; wR_2 = 0.0896	R_1 = 0.0787; wR_2 = 0.1038
Largest difference peak/hole [e Å^{-3}]	0.356/–0.423	1.056/–0.389	0.811/–0.690	0.338/–0.251

[a] $\Sigma||F_o| - |F_c||/\Sigma|F_o|$; $wR_2 = [\Sigma w(F_o^2 - F_c^2/\Sigma w(F_o^4)]^{1/2}$.

powder of **19** (0.19 g, 65%), m.p. 255–260 °C. IR (KBr): $\tilde{\nu}$ = 3100 (w), 3071 (w), 3026 (w), 2979 (w), 2952 (w), 1604 (m), 1587 (s), 1477 (m), 1442 (s), 1346 (w), 1255 (m), 1157 (w), 1112 (w), 1061 (w), 1027 (w), 849 (vs), 796 (w), 774 (s), 762 (s), 719 (w) cm^{-1}. $C_{17}H_{22}Cl_2CoN_2Si$ (412.294): calcd. C 49.52, H 5.38, N 6.79; found C 49.23, H 5.48, N 6.75. HRMS (EI): calcd. for $C_{17}H_{22}Cl_2CoN_2Si$ $[M]^+$ 411.0261; found 411.0266. μ_{eff} = 6.48 BM.

Crystal Structure Determination: Crystals were mounted in Lindemann capillaries under N_2. Diffraction data were collected with a Siemens CCD area-detector at 294(2) K with graphite-monochromated Mo-K_α radiation (λ = 0.71073 Å). A semi-empirical absorption correction was applied to the data. The structures were solved by direct methods using SHELXS-97[24] and refined against F^2 by full-matrix least squares using SHELXL-97.[25] Crystal data and experimental details of the structure determinations are listed in Table 6. CCDC-632191 to -632194 contain the supplementary crystallographic data for this paper. These data can be obtained free of charge from The Cambridge Crystallographic Data Centre via www.ccdc.cam.ac.uk/data_request/cif.

Catalytic Oligomerization of Ethylene: The oligomerization with 1 atm ethylene was carried out in a Schlenk tube. In a dried Schlenk tube was placed the pre-catalyst (5 μmol) and then the Schlenk tube was back-filled three times with N_2 and twice with ethylene. Toluene (30 mL) was added to the Schlenk tube and then the appropriate co-catalyst solution was added through a syringe. The reaction mixture was vigorously stirred at the given temperature under 1 atm ethylene. After the desired period of time (30 min or 60 min), the reaction was terminated by cooling the system to about –10 °C and then adding 10% HCl solution (30 mL). About 1 mL of the organic layer was dried with anhydrous Na_2SO_4 in a sealed Schlenk tube at about –10 °C for gas chromatographic analysis. To the remaining solution was added ethanol (100 mL), no polymer was observed. The oligomerization with 10 atm ethylene was carried out in a stainless steel autoclave (0.25 L capacity) equipped with gas ballast through a solenoid valve for continuous feeding of ethylene at constant pressure. Toluene (120 mL) containing the pre-catalyst was transferred into the fully dried reactor under N_2. The required amount of co-catalyst was injected into the reactor through a syringe. As the desired temperature was reached, the reactor was pressurized to 10 atm. After stirring for 30 min, the reactor was cooled to about –10 °C and depressurized. The contents were transferred into a cooled flask and then 10% HCl solution (30 mL) was added. The mixture was worked up and analyzed using the same procedure as described above for the 1 atm reaction.

Acknowledgments

We thank the National Natural Science Foundation of China (Grant No. 20272056) for support. We are also grateful to Professor W.-H. Sun of the Institute of Chemistry, The Chinese Academy of Sciences, for his kind help in determining the catalytic ethylene oligomerization activities of the complexes and Professors H.-B. Song and H.-G. Wang of Nankai University for single-crystal X-ray structure determinations.

[1] a) S. D. Ittel, L. K. Johnson, M. Brookhart, *Chem. Rev.* **2000**, *100*, 1169–1204; b) V. C. Gibson, S. K. Spitzmesser, *Chem. Rev.* **2003**, *103*, 283–316; c) G. J. P. Britovsek, V. C. Gibson, D. F. Wass, *Angew. Chem. Int. Ed.* **1999**, *38*, 428–447; d) S. Mecking, *Angew. Chem. Int. Ed.* **2001**, *40*, 534–540; e) S. Park, Y. Ham, S. K. Kim, J. Lee, H. K. Kim, Y. Do, *J. Organomet. Chem.* **2004**, *689*, 4263–4276; f) B. Rieger, L. S. Baugh, S. Kacker, S. Striegler (Eds.), *Late Transition Metal Polymerization Catalysts*, Wiley-VCH, Weinheim, **2003**.

[2] a) W. Keim, R. Appel, A. Storeck, C. Krüger, R. Goddard, *Angew. Chem. Int. Ed. Engl.* **1981**, *20*, 116–117; b) W. Keim, *Angew. Chem. Int. Ed. Engl.* **1990**, *29*, 235–244; c) G. Wilke, *Angew. Chem. Int. Ed. Engl.* **1988**, *27*, 185–206.

[3] a) L. K. Johnson, C. M. Killian, M. Brookhart, *J. Am. Chem. Soc.* **1995**, *117*, 6414–6415; b) L. K. Johnson, S. Mecking, M. Brookhart, *J. Am. Chem. Soc.* **1996**, *118*, 267–268.

[4] W.-H. Sun, D. Zhang, S. Zhang, S. Jie, J. Hou, *Kinet. Catal.* **2006**, *47*, 278–283, and references therein.
[5] a) M. Sauthier, F. Leca, R. F. de Souza, K. Bernardo-Gusmão, L. F. T. Queiroz, L. Toupet, R. Réau, *New J. Chem.* **2002**, *26*, 630–635; b) S. Al-Benna, M. J. Sarsfield, M. Thornton-Pett, D. L. Ormsby, P. J. Maddox, P. Brès, M. Bochmann, *J. Chem. Soc., Dalton Trans.* **2000**, 4247–4257; c) K. V. Axenov, M. Leskelä, T. Repo, *J. Catal.* **2006**, *238*, 196–205; d) S. Plentz-Meneghetti, P. J. Lutz, J. Kress, *Organometallics* **1999**, *18*, 2734–2737; e) J. Zhang, X. Wang, G.-X. Jin, *Coord. Chem. Rev.* **2006**, *250*, 95–109; f) E. Nelkenbaum, M. Kapon, M. S. Eisen, *Organometallics* **2005**, *24*, 2645–2659.
[6] a) J. Feldman, S. J. Mclain, A. Parthasarathy, W. J. Marshall, J. C. Calabrese, S. D. Arthur, *Organometallics* **1997**, *16*, 1514–1516; b) J. Zhang, Z. Ke, F. Bao, J. Long, H. Gao, F. Zhu, Q. Wu, *J. Mol. Catal. A* **2006**, *249*, 31–39; c) G. J. P. Britovsek, S. P. D. Baugh, O. Hoarau, V. C. Gibson, D. F. Wass, A. J. P. White, D. J. Williams, *Inorg. Chim. Acta* **2003**, *345*, 279–291.
[7] a) X. Tang, W.-H. Sun, T. Gao, J. Hou, J. Chen, W. Chen, *J. Organomet. Chem.* **2005**, *690*, 1570–1580; b) W.-H. Sun, X. Tang, T. Gao, B. Wu, W. Zhang, H. Ma, *Organometallics* **2004**, *23*, 5037–5047.
[8] J. Hou, W.-H. Sun, S. Zhang, H. Ma, Y. Deng, X. Lu, *Organometallics* **2006**, *25*, 236–244.
[9] a) W.-H. Sun, S. Jie, S. Zhang, W. Zhang, Y. Song, H. Ma, J. Chen, K. Wedeking, R. Fröhlich, *Organometallics* **2006**, *25*, 666–677; b) A. R. Karam, E. L. Catarí, F. López-Linares, G. Agrifoglio, C. L. Albano, A. Díaz-Barrios, T. E. Lehmann, S. V. Pekerar, L. A. Albornoz, R. Atencio, T. González, H. B. Ortega, P. Joskowics, *Appl. Catal., A* **2005**, *280*, 165–173; c) M. J. Overett, R. Meijboom, J. R. Moss, *Dalton Trans.* **2005**, 551–555; d) K. P. Tellmann, V. C. Gibson, A. J. P. White, D. J. Williams, *Organometallics* **2005**, *24*, 280–286; e) R. Schmidt, M. B. Welch, R. D. Knudsen, S. Gottfriedc, H. G. Alt, *J. Mol. Catal. A* **2004**, *222*, 17–25; f) B. L. Small, M. J. Carney, D. M. Holman, C. E. O'Rourke, J. A. Halfen, *Macromolecules* **2004**, *37*, 4375–4386; g) N. Ajellal, M. C. A. Kuhn, A. D. G. Boff, M. Hörner, C. M. Thomas, J.-F. Carpentier, O. L. Casagrande Jr, *Organometallics* **2006**, *25*, 1213–1216.
[10] a) G. J. P. Britovsek, V. C. Gibson, B. S. Kimberley, P. J. Maddox, S. J. McTavish, G. A. Solan, A. J. P. White, D. J. Williams, *Chem. Commun.* **1998**, 849–850; b) B. L. Small, M. Brookhart, A. M. A. Bennett, *J. Am. Chem. Soc.* **1998**, *120*, 4049–4050.
[11] W. Zhao, Y. Qian, J. Huang, J. Duan, *J. Organomet. Chem.* **2004**, *689*, 2614–2623, and references therein.
[12] a) Z. Weng, S. Teo, L. L. Koh, T. S. A. Hor, *Angew. Chem. Int. Ed.* **2005**, *44*, 7560–7564; b) Y. Chen, G. Wu, G. C. Bazan, *Angew. Chem. Int. Ed.* **2005**, *44*, 1108–1112; c) D. S. McGuinness, V. C. Gibson, J. W. Steed, *Organometallics* **2004**, *23*, 6288–6292; d) F. Speiser, P. Braunstein, L. Saussine, *Organometallics* **2004**, *23*, 2633–2640; e) F. Speiser, P. Braunstein, L. Saussine, *Organometallics* **2004**, *23*, 2625–2632; f) Y. Chen, R. Chen, C. Qian, X. Dong, J. Sun, *Organometallics* **2003**, *22*, 4312–4321; g) D. Sirbu, G. Consiglio, S. Gischig, *J. Organomet. Chem.* **2006**, *691*, 1143–1150; h) I. Kim, C. H. Kwak, J. S. Kim, C.-S. Ha, *App. Catal., A* **2005**, *287*, 98–107.
[13] F. Speiser, P. Braunstein, L. Saussine, *Acc. Chem. Res.* **2005**, *38*, 784–793.
[14] R. Obrecht, R. Herrmann, I. Ugi, *Synthesis* **1985**, 400–402.
[15] W.-P. Leung, H. Cheng, D.-S. Liu, Q.-G. Wang, T. C. W. Mak, *Organometallics* **2000**, *19*, 3001–3007.
[16] a) B.-J. Deelman, M. F. Lappert, H.-K. Lee, T. C. W. Mak, W.-P. Leung, P.-R. Wei, *Organometallics* **1997**, *16*, 1247–1252; b) P. B. Hitchcock, M. F. Lappert, D.-S. Liu, *J. Chem. Soc., Chem. Commun.* **1994**, 1699–1700.
[17] N. L. Allinger, X. Zhou, J. Bergsma, *J. Mol. Struct., Theochem.* **1994**, *312*, 69–83.
[18] L. P. Spencer, R. Altwer, P. Wei, L. Gelmini, J. Gauld, D. W. Stephan, *Organometallics* **2003**, *22*, 3841–3854.
[19] a) Z. Guan, W. J. Marshall, *Organometallics* **2002**, *21*, 3580–3586; b) D. P. Gates, S. A. Svejda, E. Oñate, C. M. Killian, L. K. Johnson, P. S. White, M. Brookhart, *Macromolecules* **2000**, *33*, 2320–2334.
[20] a) H.-Y. Wang, J. Zhang, X. Meng, G.-X. Jin, *J. Organomet. Chem.* **2006**, *691*, 1275–1281; b) F. Bao, R. Ma, X. Lü, G. Gui, Q. Wu, *Appl. Organomet. Chem.* **2006**, *20*, 32–38; c) S. Wu, S. Lu, *J. Mol. Catal. A: Chem.* **2003**, *198*, 29–38; d) I. Kim, C. H. Kwak, J. S. Kim, C.-S. Ha, *Appl. Catal., A* **2005**, *287*, 98–107; e) C. Carlini, M. Isola, V. Liuzzo, A. M. R. Galletti, G. Sbrana, *Appl. Catal., A* **2002**, *231*, 307–320; f) Y.-Z. Zhu, J.-Y. Liu, Y.-S. Li, Y.-J. Tong, *J. Organomet. Chem.* **2004**, *689*, 1295–1303.
[21] C. Carlini, M. Marchionna, A. M. R. Galletti, G. Sbrana, *Appl. Catal., A* **2001**, *206*, 1–12.
[22] C. Bianchini, G. Mantovani, A. Meli, F. Migliacci, *Organometallics* **2003**, *22*, 2545–2547.
[23] D. F. Evans, *J. Chem. Soc.* **1959**, 2003–2005.
[24] G. M. Sheldrick, *Acta Crystallogr., Sect. A* **1990**, *46*, 467–473.
[25] G. M. Sheldrick, *SHELXL97, Program for the refinement of crystal structures*, University of Göttingen, Göttingen, Germany, **1997**.

Received: January 7, 2007
Published Online: May 4, 2007

